Continued fraction expansion for the X-ray absorption cross section

1991 J. Phys.: Condens. Matter 3 6489

(http://iopscience.iop.org/0953-8984/3/33/024)

J. Phys.: Condens. Matter 3 (1991) 6489–6507. Printed in the UK

Continued fraction expansion for the x-ray absorption cross section

Adriano Filipponi

Università degli Studi dell' Aquila, Dipartimento di Fisica, Via Vetoio, 67010 Coppito, L'Aquila, Italy

Received 20 December 1990, in final form 18 March 1991

Abstract. The Haydock recursion scheme is for the first time applied to the matrix inversion required for calculations of x-ray absorption cross sections. A mapping of the multiple-scattering contributions into continued fraction coefficients which appears to improve the convergence of the multiple-scattering series is derived. Numerical applications to three different systems—Mn ion in water solution, a copper-imidazole molecule, and c-Si—are presented.

1. Introduction

X-ray absorption spectroscopy (XAS) is a powerful research tool in several fundamental and applied fields covering solid state and liquid physics, chemistry and molecular biology [1]. Some examples of fundamental aspects are the problems related to the approximation of the 'optical' potential felt by the photoelectron in the excited state and more generally the inclusion of many-body effects in the treatment of the process [2, 3]. Typical applications are, however, based on the possibility of obtaining local structural information around photoabsorber atoms in both the extended x-ray absorption fine structure (EXAFS) [4] and x-ray absorption near edge structure (XANES) [5] regimes.

The basic theory of XAS [6] can be easily formulated in the case of a muffin-tin model for the final state potential, where spherically symmetric atomic potentials are enclosed in non-overlapping spheres embedded in a constant interstitial region; in the following the notation of the references [7, 8] will be used. For K, L_1, ... edges the polarization averaged cross section is given by

$$\sigma(\hbar\omega) = \sigma_0 \left[\mathrm{Im} \frac{1}{\sin^2(\delta_o^{l_0})} \frac{1}{2l_0+1} \sum_{m_o} [T(I+GT)^{-1}]^{0,0}_{L_0,L_0} \right]. \qquad (1)$$

Here σ_0 is a featureless atomic cross section. T and G are the phase shifts and propagator matrices in a local basis. An element of one of these matrices is indicated by the indices i, j which span over the different atomic centres in the structure, and by a further set of angular momenta L, L' (where $L = \{l, m\}$). Each couple of atomic indices identifies an 'atomic' block of the matrices. In this representation the T-matrix is block diagonal. The propagator matrix is instead composed of null diagonal blocks,

0953-8984/91/336489+19$03.50

(i,i) sites, and non-null off-diagonal blocks $G_{i,j}^{L,L'}$ describing the free propagation from site i to site j.

$$T = \begin{pmatrix} t_0 & 0 & 0 & \dots & 0 \\ 0 & t_1 & 0 & \dots & 0 \\ 0 & 0 & t_2 & \dots & 0 \\ \vdots & \vdots & \vdots & \ddots & \vdots \\ 0 & 0 & 0 & \dots & t_{N-1} \end{pmatrix}$$

$$G = \begin{pmatrix} 0 & G_{0,1} & G_{0,2} & \dots & G_{0,N-1} \\ G_{1,0} & 0 & G_{1,2} & \dots & G_{1,N-1} \\ G_{2,0} & G_{2,1} & 0 & \dots & G_{2,N-1} \\ \vdots & \vdots & \vdots & \ddots & \vdots \\ G_{N-1,0} & G_{N-1,1} & G_{N-1,2} & \dots & 0 \end{pmatrix}. \tag{2}$$

In the present choice of the potential the phase-shift matrix for the atom i is diagonal in the L indices, $t_i^{L,L'} = t_i^l \delta_{L,L'}$ because the angular momentum is conserved in the scattering from a single site, due to the spherical symmetry of the potential in the atomic sphere.

The expression for a single propagator block involves $3J$ symbols and is given by

$$G_{i,j}^{L,L'} = -(4\pi(2l+1)(2l'+1))^{\frac{1}{2}} \sum_{l_1} (2l_1+1)^{\frac{1}{2}} \begin{pmatrix} l & l' & l_1 \\ 0 & 0 & 0 \end{pmatrix} \times \begin{pmatrix} l & l' & l_1 \\ m & -m' & m'-m \end{pmatrix} (-1)^{m'} h_{l_1}^{+}(k\rho_{ij}) Y_{l_1,m'-m}(R_{i,j}). \tag{3}$$

Here h_l^+ are the Hankel functions, and $Y_{l,m}$ are the spherical harmonics. Under exchange of indices $i,j \to j,i$ the spherical harmonic changes as $Y_{lm} \to (-1)^l Y_{l,m}^*$ due to the inversion of the propagation direction. We note that the propagator matrix G and the $(I+GT)$ matrices result in general complex matrices.

The exact calculation of the cross section requires a few elements of the inverse of the matrix $I+GT$ in equation (1) to be computed, corresponding to the photoabsorber site and angular momentum $L_0 = \{l_0, m_0\}$. For the previously mentioned edges $l_0 = 1$ due to the dipole selection rule.

The inversion is usually performed numerically and possibly using some approximate method which is fast in computing time and provides a simple physical interpretation of the successive approximations. Two kinds of approach, which are connected with two different energy limits, have so far been proposed. In the low energy limit, where the Hankel functions have a larger modulus, all of the atoms are strongly coupled by the G-matrix. As a consequence the effects of particular structural arrangements on the cross section can hardly be decoupled. Only the total contribution from the whole structure has a meaning. Successful methods for performing the total inversion which are commonly used nowadays in XANES calculations have been proposed by Durham *et al* and Vvedensky *et al* [9]. These methods take advantage of a partition of the original cluster into progressively successive shells and make use of the Gauss–Seidel–Aitken iterative method to perform the basic inversion.

In the high energy region the matrix inversion can be performed by series, each term of which represents successive scattering by a sequence of sites [6, 8]. The physical

picture is particularly appealing but unfortunately this multiple scattering (MS) series may not converge in the low energy limit.

In this paper a new way of approximating the matrix inversion in terms of continued fraction (CF) approximants is worked out, adapting, to the XAS case, ideas which have been extensively applied to other areas of the solid state and also statistical physics. Both analytical and numerical results will be presented.

The plan of the paper is the following. In section 2.1 the standard MS expansion is reviewed. In section 2.2 the Haydock recursion is introduced and applied analytically to the calculation of the cross section. In section 2.3 the CF coefficients are explicitly derived up to the third order as a function of the MS terms and the meaning of the successive approximants is discussed. In section 2.4 the problem of convergence of the CF approach is treated at a qualitative level. Finally section 3 contains examples of explicit numerical calculations.

2. Theory

2.1. Multiple scattering approach

In the high energy limit the GT matrix gives a small contribution with respect to I in the inversion, and the formal matrix expansion $T(I+GT)^{-1} = T(I - GT + GTGT - GTGTGT + \ldots)$ is convergent [8]. Of this expansion only the diagonal terms corresponding to the photoabsorber atom at the initial angular momentum should be evaluated. If the block nature of T and G is also taken into account, it is realized that the TGT term gives no contributions. The (MS) series is then given by

$$\sigma(\hbar\omega) = \sigma_0 \left[\mathrm{Im} \frac{t_o^{l_0}}{\sin^2(\delta_o^{l_0})} \frac{1}{2l_0+1} \sum_{m_0} (1 + \xi_2 + \xi_3 + \xi_4 + \cdots) \right] \tag{4}$$

where

$$\xi_2(m_0) = \sum_{i=1}^{N-1} (G_{0,i} t_i G_{i,0} t_0)_{L_0,L_0} \tag{5a}$$

$$\xi_3(m_0) = -\sum_{j=1}^{N-1} \sum_{\substack{i=1 \\ (i\neq j)}}^{N-1} \left[G_{0,j} t_j G_{j,i} t_i G_{i,0} t_0 \right]_{L_0,L_0} \tag{5b}$$

$$\xi_4(m_0) = \sum_{k=1}^{N-1} \sum_{\substack{j=0 \\ (j\neq k)}}^{N-1} \sum_{\substack{i=1 \\ (i\neq j)}}^{N-1} \left[G_{0,k} t_k G_{k,j} t_j G_{j,i} t_i G_{i,0} t_0 \right]_{L_0,L_0} . \tag{5c}$$

These complex ξ_n quantities are related to the more commonly used χ_n oscillations by the expression

$$\chi_n = \mathrm{Im} \left(\frac{t_o^{l_0}}{\sin^2(\delta_o^{l_0})} \frac{1}{2l_0+1} \sum_{m_0} \xi_n(m_0) \right) . \tag{6}$$

At sufficiently high photoelectron energy the matrix GT gives a small contribution and consequently the first non-trivial terms account for all of the signal. In this region

(EXAFS) [4] the expansion reads $1 + GTGT + O(GT^3) \rightarrow 1 + \xi_2$. In ξ_2 the only possible products of G and T are related to scattering paths involving only one atom i at a time. The structural signal is therefore decoupled in the sum of the atomic contributions which can be more easily analysed. In the region closer to the edge where more MS terms are needed to describe the signal correctly it is not easy to associate spectral features to particular structural arrangements. Progress on this line within the framework of the MS theory has been recently obtained in which the XAS signal is expressed in terms of averages over the n-particle distribution functions [10].

This MS expansion is particularly satisfactory because it provides a direct physical interpretation of the successive terms, unfortunately the so called intermediate MS [8] region is usually narrow due to convergence problems at lower energies.

2.2. Recursion method

A different algorithm that appears to be particularly suitable for calculating the elements of the inverse of the $I + GT$ matrix in equation (1) is the Haydock recursion scheme. The method comprises a powerful recursive algorithm that can be applied to a generic matrix A in order to calculate any diagonal element of its inverse, for instance $(A^{-1})_{1,1}$. Initially, a transformation of the given matrix into tridiagonal form by means of the following recursive relations (originally introduced by Lanczos [14]) is performed.

$$b_{n+1}|n+1\rangle = A|n\rangle - a_n|n\rangle - b_n|n-1\rangle \tag{7a}$$

$$b_{n+1}\langle n+1| = \langle n|A - a_n\langle n| - b_n\langle n-1|. \tag{7b}$$

The vectors $|n\rangle$ and $\langle n|$ represent a biorthonormal basis set $\langle n|m\rangle = \delta_{n,m}$ in which the matrix A is tridiagonal. By definition, the coefficients a_n and b_n are

$$a_n = \langle n|A|n\rangle \qquad b_{n+1} = \langle n+1|A|n\rangle = \langle n|A|n+1\rangle. \tag{8}$$

Now, the seed for the recursive relation (7) is chosen as the vector with all null elements besides a unity element in a position corresponding to the diagonal element of A^{-1} that is to be calculated. Then, by construction, the diagonal element of the inverse matrix is equal to the diagonal element in position $(1, 1)$ of the inverse of the tridiagonal matrix. This element can be obtained by means of the following continued fraction expansion:

$$(A^{-1})_{1,1} = \cfrac{1}{a_1 - \cfrac{b_1^2}{a_2 - \cfrac{b_2^2}{a_3 - \cfrac{b_3^2}{a_4 - \ddots}}}} \tag{9}$$

whose coefficients are directly given by equation (8) and (7). Progressively more accurate expressions for the element of the inverse matrix can be obtained by the successive approximants of the continued fraction, and consequently performing successive recursion steps.

This method has been widely used in several areas of solid state physics since many expressions involving Green's functions in a local basis reduce to the calculation of

some elements of an inverse. Pioneering works in this field were mainly by Haydock, Heine and Kelly [11, 12]. Very similar procedures are also used in the different context of non-equilibrium statistical mechanics related to the memory function approach; a full overview of this field of research can be found in [13]. In typical cases the recursion method is applied once for all energies to the calculation of the resolvent $(E-H)^{-1}$ of a Hamiltonian H in a local basis. The application of the recursion method that will be presented here is of a different nature; indeed the method will be used to perform the inversion of the matrix $I+GT$ in equation (1) which is tridiagonalized again for each new energy value. The version of the algorithm needed in this case is that for a generic complex matrix; it is slightly more complicated than the more usual one for symmetric or Hermitian matrices because it is necessary to operate with the matrix both to the right and to the left. For further details on this algorithm see for instance [15].

The fundamental quantities of interest will be the expressions of the type $[(I+GT)^{-1}]^{0,0}_{L_0,L_0}$ that have to be evaluated for each energy point at the various m_0 quantum numbers, for instance $m_0=-1,0,1$. The MS expansion for such quantities will be the $(1+\xi_2(m_0)+\xi_3(m_0)+\xi_4(m_0)+\cdots)$ expressions in equation (4). For each diagonal element of the inverse a different recursion procedure will be performed starting from the appropriate vector obtaining a suitable continued fraction expansion. Later we will focus on a single recursion.

In order to give a physical interpretation to the successive approximants of the continued fraction we work out analytically the recursion method in the general case of a system with N atomic sites. Following the previous notation, vectors and matrices will be indicated in block format, each block referring to one atom. The internal indices of the block will be l, m, i.e. a set of angular momenta sufficient to describe the scattering from the site. The starting vector is defined by the element corresponding to atom 0 and angular momenta l_0, m_0. If the average over several m_0 values were needed, several continued fractions will have to be calculated each one starting from the appropriate m_0 element. The null block vector will be indicated with $\underline{0}$ while the one with the only non-zero element equal to 1 in position l_0, m_0 will be $\underline{l}$. Then the starting vectors are:

$$|1\rangle = \begin{pmatrix} \underline{l} \\ \vdots \\ \underline{0} \\ \vdots \end{pmatrix} \qquad \text{and} \qquad \langle 1| = (\underline{l}, \ \ldots, \ \underline{0}, \ \ldots) \tag{10}$$

clearly $a_1 = \langle 1|(I+GT)|1\rangle = 1$. By applying the matrix to the vectors and subtracting the component along $|1\rangle$ one obtains the vectors of the second step:

$$b_1|2\rangle = (I+GT-a_1)|1\rangle = \begin{pmatrix} \underline{0} \\ \vdots \\ (G_{j,0}t_0)_{L,L_0} \\ \vdots \end{pmatrix} \tag{11a}$$

and

$$b_1\langle 2| = \langle 1|(I+GT-a_1) = (\underline{0}, \ \ldots, \ (G_{0,j}t_j)_{L_0,L}, \ \ldots). \tag{11b}$$

$G_{i,j}t_j$ indicates a row by column product in the angular momentum indices; in this case it has to be evaluated for fixed L_0 and running L. The complex number b_1 is by definition

$$b_1^2 = \sum_{i=1}^{N-1} (G_{0,i}t_i G_{i,0}t_0)_{L_0,L_0} = \xi_2 \tag{12}$$

i.e. it coincides with the expression for the second term in the MS expansion. By acting with $I + GT$ on the vector $|2\rangle$ we obtain

$$(I+GT)|2\rangle = \frac{1}{b_1} \begin{pmatrix} \sum_{i=1}^{N-1} (G_{0,i}t_i G_{i,0}t_0)_{L,L_0} \\ \vdots \\ (G_{j,0}t_0 + \sum_{\substack{i=1 \\ (i\neq j)}}^{N-1} G_{j,i}t_i G_{i,0}t_0)_{L,L_0} \\ \vdots \end{pmatrix} \tag{13}$$

here j runs over the atoms $1, \ldots, N-1$. The a_2 coefficient is readily calculated:

$$a_2 = \frac{1}{b_1^2} \left[\sum_{i=1}^{N-1} G_{0,i}t_i G_{i,0}t_0 + \sum_{j=1}^{N-1} \sum_{\substack{i=1 \\ (i\neq j)}}^{N-1} G_{0,j}t_j G_{j,i}t_i G_{i,0}t_0 \right]_{L_0,L_0} = 1 - \frac{\xi_3}{\xi_2}. \tag{14}$$

The last equality is obtained by identifying the first $GtGt$ product clearly as the ξ_2 previously defined and the second $GtGtGt$ product as the third term in the MS series (ξ_3) where all the possible scattering events of the type 0–i–j–0 are included.

Let us now proceed to the next terms first of all evaluating

$$\langle 2|(I+GT) = \frac{1}{b_1} \left(\sum_{i=1}^{N-1} (G_{0,i}t_i G_{i,0}t_0)_{L_0,L}, \cdots, \right.$$
$$\left. (G_{0,j}t_j + \sum_{\substack{i=1 \\ (i\neq j)}}^{N-1} G_{0,i}t_i G_{i,j}t_j)_{L_0,L}, \cdots \right). \tag{15}$$

Now the vectors $|3\rangle$ and $\langle 3|$ are obtained by orthogonalization to the first two:

$$b_2|3\rangle = (I+GT)|2\rangle - a_2|2\rangle - b_1|1\rangle = \frac{1}{b_1} \left[\begin{pmatrix} \sum_{i=1}^{N-1} (G_{0,i}t_i G_{i,0}t_0)_{L,L_0} \\ \vdots \\ (G_{j,0}t_0 + \sum_{\substack{i=1 \\ (i\neq j)}}^{N-1} G_{j,i}t_i G_{i,0}t_0)_{L,L_0} \\ \vdots \end{pmatrix} \right.$$
$$\left. - \left(1 - \frac{\xi_3}{\xi_2}\right) \begin{pmatrix} \underline{0} \\ \vdots \\ (G_{j,0}t_0)_{L,L_0} \\ \vdots \end{pmatrix} - \xi_2 \begin{pmatrix} \underline{1} \\ \vdots \\ \underline{0} \\ \vdots \end{pmatrix} \right] \tag{16a}$$

and the two terms $G_{j,0}t_0$ can be summed and the coefficients will be ξ_3/ξ_2. Similarly

$$b_2\langle 3| = \langle 2|(I+GT) - a_2\langle 2| - b_1\langle 1| = \frac{1}{b_1}\left(\sum_{i=1}^{N-1}(G_{0,i}t_iG_{i,0}t_0)_{L_0,L} - \xi_2\delta_{L_0,L}, \ldots,\right.$$
$$\left.\left(\frac{\xi_3}{\xi_2}G_{0,j}t_j + \sum_{\substack{i=1\\(i\neq j)}}^{N-1} G_{0,i}t_iG_{i,j}t_j\right)_{L_0,L}, \ldots\right). \tag{16b}$$

The normalizing factor is easily computed,

$$b_2^2 = \frac{1}{b_1^2}\left(\sum_{i,j=1}^{N-1}(G_{0,i}t_iG_{i,0}t_0G_{0,j}t_jG_{j,0}t_0) - \xi_2^2 - \frac{\xi_3^2}{\xi_2}\right.$$
$$\left. + \sum_{\substack{i,j,k=1\\i\neq j\neq k}}^{N-1}(G_{0,i}t_iG_{i,j}t_jG_{j,k}t_kG_{k,0}t_0)\right)_{L_0,L_0} = \frac{1}{\xi_2}(\xi_4 - \xi_3^2/\xi_2 - \xi_2^2). \tag{17}$$

The first and last terms in the previous sum are recognized to add up to the ξ_4 term of the MS series, indeed in the second one all the paths 0–i–j–k–0 with $j \neq 0$ are included while the 0–i–0–k–0 terms are represented by the first sum.

Acting again with matrix $I+GT$ on vector $|3\rangle$ we obtain:

$$(I+GT)|3\rangle = \frac{1}{b_1b_2}\begin{pmatrix} \displaystyle\sum_{i=1}^{N-1}(G_{0,i}t_iG_{i,0}t_0)_{L,L_0} - \xi_2\delta_{L,L_0} \\ \displaystyle + \sum_{j=1}^{N-1}\left[G_{0,j}t_j\left(\frac{\xi_3}{\xi_2}G_{j,0}t_0 + \sum_{\substack{i=1\\(i\neq j)}}^{N-1}G_{j,i}t_iG_{i,0}t_0\right)\right]_{L,L_0} \\ \vdots \\ \left[G_{k,0}t_0\displaystyle\sum_{i=1}^{N-1}(G_{0,i}t_iG_{i,0}t_0)\right]_{L,L_0} + \left(\frac{\xi_3-\xi_2^2}{\xi_2}\right)(G_{k,0}t_0)_{L,L_0} \\ \displaystyle + \left(1+\frac{\xi_3}{\xi_2}\right)\sum_{\substack{i=1\\(i\neq k)}}^{N-1}(G_{k,i}t_iG_{i,0}t_0)_{L,L_0} \\ \displaystyle + \sum_{\substack{j=1\\(j\neq k)}}^{N-1}\sum_{\substack{i=1\\(i\neq j)}}^{N-1}(G_{k,j}t_jG_{j,i}t_iG_{i,0}t_0)_{L,L_0} \\ \vdots \end{pmatrix} \tag{18}$$

where the atom row index is now k. After a simple algebra we obtain the a_3 coefficient.

$$a_3 = \langle 3|I+GT|3\rangle = \frac{1}{b_1^2b_2^2}\left\{-\xi_2^2 - 2\frac{\xi_3^2}{\xi_2} + \left(1+2\frac{\xi_3}{\xi_2}\right)\left(\sum_{i\neq j}(G_{0,i}t_iG_{i,0}t_0G_{0,j}t_jG_{j,0})\right.\right.$$
$$\left.\left. + \sum_{\substack{i,j,k\\(i\neq j\neq k)}}(G_{0,k}t_kG_{k,j}t_jG_{j,i}t_iG_{i,0})\right)_{L,L_0}$$

$$+\left[\sum_{\substack{i,j,k,l=1\\(i\neq j\neq k\neq l)}}^{N-1}(G_{0,k}t_kG_{k,j}t_jG_{j,i}t_iG_{i,l}t_lG_{l,0}t_0)\right.$$

$$+\sum_{\substack{i,j,k=1\\(k\neq j}}^{N-1}((G_{0,k}t_kG_{k,j}t_jG_{j,0}t_0G_{0,i}t_iG_{i,0}t_0)$$

$$\left.+(G_{0,i}t_iG_{i,0}t_0G_{0,j}t_jG_{j,k}t_kG_{k,0}t_0))\right]_{L,L_0}\Bigg\}$$

$$=\frac{1}{b_1^2b_2^2}\left[-\xi_5+\xi_4\left(1+2\frac{\xi_3}{\xi_2}\right)-\frac{\xi_3^2}{\xi_2}\left(1+\frac{\xi_3}{\xi_2}\right)-\xi_2^2\right]. \tag{19}$$

The last equality is obtained by recognizing that the sums with four and five Gt products add up to the total fourth and fifth order MS. Indeed the possible paths involving the photoabsorber atom as second or fourth scattering site are listed separately. Although tedious the derivation can be continued to higher orders with increasing algebraic difficulties.

The present treatment has led to explicit expressions for the coefficients of the tridiagonal matrix, up to the third order, in terms of the MS contributions ξ_j.

2.3. Continued fraction expansion

The formulae which have been derived earlier are of a particular interest for practical as well as theoretical reasons. By using the Lanczos–Haydock recursion we have obtained a transformation of the original matrix into tridiagonal form ($\{a_n, b_n\}$). These expressions provide the mapping of the original system of n atomic centres that scatter in many angular momentum channels into a simple one-dimensional chain where the scattering can occur between successive degrees of freedom only. This is the well known 'chain model' [11–13]. In figure 1 a pictorial representation of the effect of the transformation is shown.

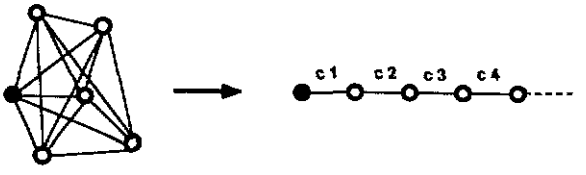

Figure 1. Schematic representation of the mapping of the original system (left) with a strong coupling among all of the sites into the chain model (right) in which the coupling is reduced to neighbouring sites only.

The diagonal element of the inverse of the $I + GT$ matrix, which is our unknown, equals the $(1, 1)$ element of the inverse of the tridiagonal matrix which is much easier to calculate. The element $(1, 1)$ of the tridiagonal matrix a_1 is unity, the other are the previously calculated a_j, $j \geq 2$. It is possible to transform the tridiagonal matrix $\{a_n, b_n\}$ into a tridiagonal matrix $\{1, c_n\}$ (with all 1s on the main diagonal) without

affecting the $(1,1)$ element of the inverse. This is obtained as follows

$$\begin{pmatrix} a_1 & b_1 & & \\ b_1 & a_2 & b_2 & \\ & b_2 & a_3 & \ddots \\ & & \ddots & \ddots \end{pmatrix} \rightarrow \begin{pmatrix} 1 & c_1 & & \\ c_1 & 1 & c_2 & \\ & c_2 & 1 & \ddots \\ & & \ddots & \ddots \end{pmatrix} \tag{20}$$

where $c_i = b_i/\sqrt{a_i a_{i+1}}$. This transformation corresponds to an equivalence transformation on the related continued fraction. In terms of the ξ_n the c_i coefficients are respectively:

$$c_1 = \frac{\xi_2}{\sqrt{\xi_2 - \xi_3}} \qquad c_2 = \frac{\xi_4 - \xi_2^2 - \xi_3^2/\xi_2}{\sqrt{(\xi_2 - \xi_3)(-\xi_2^2 - \xi_3^2(\xi_2 + \xi_3)/\xi_2^2 + (1 + 2\xi_3/\xi_2)\xi_4 - \xi_5}}.$$

It can be argued that, because of the reduced coupling between the various degrees of freedom, the convergence properties of any approximate evaluation of the inverse will be largely improved by this transformation. The simplest way to calculate the $(1,1)$ element of the inverse matrix consists in the continued fraction expansion [11]. A truncation of the tridiagonal matrix at the nth order will correspond to approximate the continued fraction with its nth approximant. In our case the continued fraction approximants hereafter indicated by f_n can be given as a function of the MS terms, using the coefficients (a_n, b_n) previously calculated. The first of them are

$$f_1 = 1 \qquad f_2 = \cfrac{1}{1 - \cfrac{\xi_2}{(1 - \xi_3/\xi_2)}}$$

$$f_3 = \cfrac{1}{1 - \cfrac{\xi_2}{(1 - \xi_3/\xi_2) - \cfrac{\frac{1}{\xi_2}(\xi_4 - \xi_2^2 - \xi_3^2/\xi_2)}{\cfrac{[-\xi_5 + \xi_4(1 + 2\xi_3/\xi_2) - \xi_3^2/\xi_2(1 + \xi_3/\xi_2) - \xi_2^2]}{(\xi_4 - \xi_2^2 - \xi_3^2/\xi_2)}}}}. \tag{21}$$

These approximants are progressively more cumbersome expressions for the quantities $[(I + GT)^{-1}]^{0,0}_{L_0,L_0}$, which involve a finite number of terms of the MS series.

A similar mapping of the MS series into CF can actually be obtained using recursive relations involving Hankel determinants (see for instance [16]), which can map any power series into a CF. However by direct inspection it is found that such CF approximants are effectively different from those obtained by the recursion method in this specific case.

The physical meaning of the continued fraction approximants f_n is evident; they correspond to calculate exactly the cross section for a finite chain model which includes $n-1$ bonds. Each bond of the chain model is an effective coupling including a very large number of scattering events in the real system which involve all of the atoms. In principle one could perform the inversion of the tridiagonal matrix by series obtaining a modified MS series, the CF approximants represent the sum of the series related to a finite chain model.

In order to understand the relation between CF approximants and MS series it is also instructive to expand the approximants. It is recognized that by ordering the

various terms according to the index m in the ξ_m for a generic approximant f_n we obtain

$$f_n = 1 + \xi_2 + \xi_3 + \ldots + \xi_n + O(n+1). \tag{22}$$

The terms up to order n coincide with the terms of the MS series but in addition corrective terms of any order are present. These are expressions such as the products and powers of ξ_m terms, with $m \leqslant n$, that in some cases can be associated with leading terms of the exact MS series. Thus the addition of one a or b coefficient to the continued fraction corresponds to reproducing a new term of the MS series correctly.

The formulae presented in this and in the previous sections are remarkable for two reasons at least. The recursion method represents an alternative algorithm to perform numerically the matrix inversion, that can be easily implemented, which requires $O(N^2)$ operations and can be used in direct calculations of XANES spectra or even to calculate XAS spectra in a more extended energy interval. The analytic procedure presented in section 2.2 clarifies what really happens in such a numerical implementation and what are the connections with the MS expansion. We note, for instance, that the high energy limit of the approximants coincide with the EXAFS single scattering terms. Numerical application of the recursion algorithm will be presented in section 3.

From a different point of view the present treatment provides a systematic algorithm to map a finite number of MS terms into continued fraction coefficients. This can be in principle implemented easily calculating the complex MS terms ξ_n using methods like that of [8] or similar procedures, and including such terms in the expressions (21) for f_n. In the next sections we will show how that can result in an improvement in the convergence, thus providing a better and stable approximation to the cross section, a particularly relevant occurrence in the region where the MS series is not convergent at all. Expressions like equation (21) may represent a bridge between the usual treatment of the high energy EXAFS region and the edge XANES region.

2.4. Convergence

The mathematical theory of continued fractions is well developed and details on convergence theorems, truncation errors and numerical stability can be found in books [17]. A discussion of the convergence properties of the CF generated by the Haydock recursion scheme applied to typical density of states or memory function problems can be found in [12] and [13].

In this section the convergence of the CF algorithm applied to the inversion of the $I + GT$ matrix is discussed. The results presented here stimulate further work of a more rigorous nature on the subject.

If the original matrix is finite dimensional with size N (a system with a finite number of atoms and using a finite number of angular momenta) the Haydock recursion scheme is exact in N steps and the corresponding CF is finite. In this case what should be considered is the truncation error obtained if the procedure is stopped at step $m < N$.

The problem can be stated as follows: let us map the continued fraction approximants f_n into the difference series (or sum)

$$f_\infty = f_1 + (f_2 - f_1) + (f_3 - f_2) + \ldots + (f_n - f_{n-1}) + \ldots. \tag{23}$$

The recursion method will be said to converge if the rest of the difference series can be reduced to an arbitrary small number. The rest in modulus can be overestimated by

$$|f_N - f_n| \leqslant \sum_{i=n+1}^{N} |(f_i - f_{i-1})|. \tag{24}$$

In the case of a tridiagonal matrix of the type $\{1, c_n\}$ it is possible to obtain the following simple recursion relation between successive differences of approximants.

$$[f_{n+1} - f_n] = [f_n - f_{n-1}] \left(\frac{D^n}{D^{n+1}} - 1 \right). \tag{25}$$

Here D^n and D^{n+1} are the determinants of the tridiagonal matrix truncated at the order n and $n+1$ respectively. Iterating equation (25) it is possible to express any difference of approximants as a function of a fixed difference with lower indexes, and therefore the rest as a function of the last calculated difference.

$$(f_N - f_n) = (f_n - f_{n-1}) \times E \qquad E = \left(\sum_{M=n+1}^{N} \prod_{i=n+1}^{M} \gamma_i \right)$$

where

$$\gamma_i = \left(\frac{D^n}{D^{n+1}} - 1 \right). \tag{26}$$

Provided that we start from some n value for which all the γ_i have a modulus less than unity then the rest is finite (an upper limit can be calculated), and the CF converges. For instance let $|\gamma_i| \leqslant \Gamma < 1$, $i > n$, then

$$|(f_N - f_n)| \leqslant |(f_n - f_{n-1})| \times \left| \frac{1 - \Gamma^{N-n}}{1 - \Gamma} \right| \leqslant |(f_n - f_{n-1})| \times \left| \frac{1}{1 - \Gamma} \right|. \tag{27}$$

Thus the 'convergence' criterion in terms of the chain model determinants is

$$\Gamma = \max_{i \in n+1, N} \left| \left(\frac{D^i}{D^{i+1}} - 1 \right) \right| < 1 \tag{28}$$

starting from some finite n value which is equivalent to

$$\mathrm{Re} \left(\frac{D^{i+1}}{D^i} \right) > \frac{1}{2} \qquad i > n. \tag{29}$$

This is a condition on the ratio of the chain model determinants with $i+1$ and i sites for $i > n$. In terms of the eigenvalue spectrum of the $\{1, c_n\}$ matrix, equation (29) will be satisfied if, for instance, after a given size n adding new bonds on the chain does not change the old eigenvalues too much and will only add new eigenvalues close to $(1, 0)$.

Now it will be of a particular interest to establish convergence criteria in terms of some properties of the original matrix $I + GT$. If $GT = 0$ the matrix is the identity

and clearly the procedure will converge at the first step. Increasing the magnitude of the GT matrix the eigenvalues of $I + GT$ will spread around the $(1,0)$ point and in general more recursion steps will be needed. The fundamental reason for convergence of the procedure is that the Haydock recursion scheme automatically selects as first basis elements the directions corresponding to the eigenvalues of the original matrix which mostly depart from their centre $(1,0)$. For this reason once the 'dangerous' directions have been selected condition (29) will be satisfied. Therefore the number of iterations required will be of the order of the number of dangerous eigenvalues.

In terms of the spectrum of the original matrix, a very coarse condition can be obtained substituting the determinant ratio of the $\{1, c_n\}$ matrix in equation (29) with a generic eigenvalue of the $I + GT$ matrix. An estimate of the number of required iterations is given by the number of eigenvalues out of the region $\mathrm{Re}(\lambda) > \frac{1}{2}$. If this number is finite the CF algorithm is convergent.

This statement is approximate because the two spectra do not coincide due to the non-unitarity of the transformation although their centre is the same $(1,0)$ point. The condition is however approximate by its own nature and establishes only an estimate of the required number of iterations. The CF algorithm is therefore expected to converge in the cases of systems with a finite number of atoms. Indeed the number of dangerous eigenvalues will be finite even though the limit of angular momenta is extended to large values; only trivial eigenvalues will be added and the spectrum will accumulate around the $(1,0)$ point. Problems may arise in the limit of infinite number of atoms because the eigenvalues may coalesce into a cut or equivalently an infinite number of them may lay in the dangerous region.

In comparison with the condition for convergence of the MS series which requires all eigenvalues to be within the circle of radius 1 centred around $(1,0)$ in the complex plane ($\lambda_j \in \{|\lambda_j - 1| < 1\}$) the convergence requirement for the CF algorithm is less stringent. Indeed an infinite number of dangerous eigenvalues is now required, while to prevent the MS series converging a single eigenvalue is sufficient.

In the next section examples of eigenvalue spectra of typical matrices and the related number of iterations needed will be given.

3. Numerical examples

In this section numerical applications of the recursion method will be presented. Let us first point out that both the brute force numerical application of the recursion to the matrix $I + GT$ and the wiser substitution of the ξ_n terms in equation (21) are perfectly equivalent. The latter method is faster but in practice can only be used up to the f_3 approximant because of the complexity of calculating higher order ξ_n terms. The former method turned out to be more practical and the examples presented in the following will refer to this procedure. From the computing time point of view the recursion method is economical with time and memory. At each step the number of operations is of the order of N^2, N being the dimension of the matrix which is $\sum_i (l^i_{\max} + 1)^2$; $l^i_{\max}$ is the maximum angular momentum used to describe the scattering from the site i of the system, the sum is extended to all of the atoms. Two numerical tricks can be easily implemented to speed up the computation. The first consists in considering the $l_{\max}$ atom to be energy dependent as well; indeed the angular momenta effective in the scattering increase as $l_{\max} \approx k * R_c$ where R_c is some effective radius of the potential and $k \sim \sqrt{E}$ is the photoelectron wavevector,

where E is the energy above the muffin-tin level. In this way it is possible to reduce the matrix dimension and computing time considerably in the low-energy part of the spectrum. In the high-energy part of the spectrum large matrices are needed; however, the energy mesh can be coarser because the cross section varies smoothly. The second trick consists in using all the possible symmetries of the atomic cluster to reduce the number of non-zero elements in the G matrix. Even if the system has no symmetries it is always possible to orient the (say) $\hat{z}$-axis along the 0–1 bond for instance obtaining the $G_{0,1}$ propagator diagonal on the m indices. When many zeroes are present in the GT matrix the computing time is reduced because only the products of the non-zero elements can be performed at each step. If the GT matrix can be reduced in diagonal form blocks, than only the block of the $0, L_0$ element will play a role in the recursion, and therefore its dimension is considerably reduced.

The applications that will be presented here cover different systems in order to show the generality of the method. All of the calculations use a complex, energy-dependent, Hedin–Lundqvist potential [2, 3], in the muffin-tin approximation. The phase shifts have been generated using the routines mainly written by Natoli and Tyson, included in the GNXAS package [18]. The program to compute the XAS using the CF approach has been written by the author. No explicit use of the symmetry has been made in the calculation that will be presented. It is clear that working using a symmetrized basis larger problems than those treated here can be handled. The CF method, however, enables even clusters without any symmetry of the size of 100 atoms to be treated.

The spirit of this paper is to assess the theoretical aspect rather than present extended applications to model systems; for this reason no attempts have been made to improve the modelling of the potential. Neither have configurational damping nor core–hole lifetime effects been taken into account. For each application an appropriate experimental reference will be quoted for comparison. The experimental spectra are not reproduced in the figures. Clearly all of the calculated spectra coincide, within the convergence errors, with those obtained using a standard XANES calculation.

The first system chosen is a simple cluster with a Mn atom (photoabsorber) in the centre surrounded by six oxygen atoms in an octahedral configuration at a distance of 2.17 Å. This geometry is representative of the water configuration of transition metal ions in solution. The MnO_6 complex has been the subject of many XANES and MS studies [8, 19]. The calculated cross section as a function of the energy up to 15 Ryd above the absorption edge is reported in figure 2 for an increasing number of iterations from two to six. Here 'number of iterations' is intended to be the dimension of the resulting CF, or equivalently the number of the sites in the chain model.

The fast convergence of the algorithm even in the edge region is evident; in the last spectrum the relative error is less than 10^{-5}, but the correct shape, similar to more standard XANES calculations, is reached since the third iteration which corresponds to the f_3 analytical expressions reported in section 2.3 equation (21). By comparison the MS series up to the fourth order [8] is still not sufficient in the first 2–3 Ryd.

The comparison with the experiment [8] should be regarded with some caution because no configurational damping has been considered; however all of the features are well reproduced.

The convergence properties of the calculation depend strongly on the spectrum of the $I + GT$ matrix which is shown in figure 3 for different energy values. The eigenvalues, which are indicated by dots on the complex plane, have been calculated numerically, in this and in the successive cases, using the full $I + GT$ matrix; they

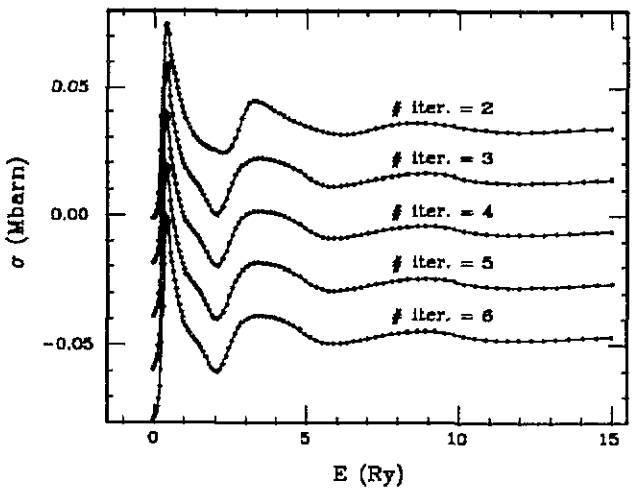

Figure 2. Absorption cross section for the MnO_6 complex calculated with the recursion method and using two, three, four, five and six iterations. A chain model with three sites is sufficient to reproduce correctly the near-edge shape, while two are certainly sufficient for the EXAFS region. With six iterations the relative error is less then 10^{-5} in all of the energy range.

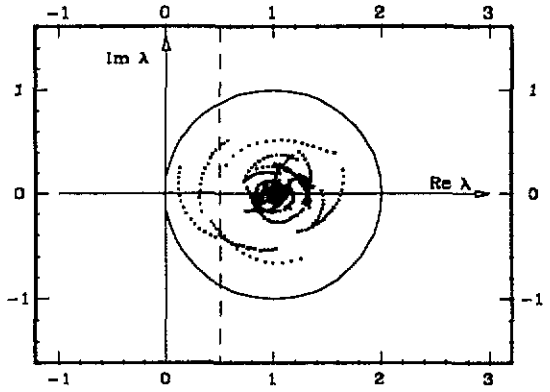

Figure 3. Behaviour of the eigenvalues of the $I + GT$ matrix for the MnO_6 complex has a function of the energy. The eigenvalue spiral in anticlockwise sense around the (1,0) point of the complex plane as the energy increases. They are always enclosed within the convergence circle for the MS series.

spiral in an anticlockwise sense around the point $(1, 0)$ as the energy increases. We see that in this case all of the eigenvalues lay within the circle of radius 1 from the $(1, 0)$ point, that is the MS series is always convergent. However at low energy there are at least two dangerous eigenvalues with a modulus close to the circle boundary on the left side of the plot which make the convergence of the MS series slow. When the energy increases these eigenvalues quickly move toward the $(1, 0)$ point and the convergence problems are reduced for the MS series. The vertical broken line in figure 3 represents the $\mathrm{Re}(z) = \frac{1}{2}$ line. Because of the small number of eigenvalues on the left-hand side (≈ 2) it is expected the the CF algorithm converges in a few iterations as it, in fact, does.

This example shows the power of the method in the case of small molecules with a single coordination shell. Even if the symmetry is not taken into account, the whole spectrum can be calculated in a few CPU seconds on minicomputers.

In the following examples only the converged results will be presented. As a practical criterion the convergence was tested by the modulus of the difference of successive approximants of the continued fraction. When this number was less than 10^{-5} the iteration was stopped.

The second example of an application is a biological molecule: Diperchlorato-tetraimidazolo-copper(II), containing four imidazole rings around a Cu atom. The imidazole ring is known to produce strong MS effects in the extended energy region [20]. The present total calculation includes 21 atoms of the structure and covers the range for the photoelectron wavevector $k = 2$–10 Å^{-1}. The relative oscillation of the cross section multiplied by k^3 is reported in figure 4 in a scale that can be easily compared with the experiment [20]. The calculation matches the experiment in a detailed fashion, apart from the amplitude of the signal and its high frequency contributions especially at high k values due to the lack of a configurational average in the calculation.

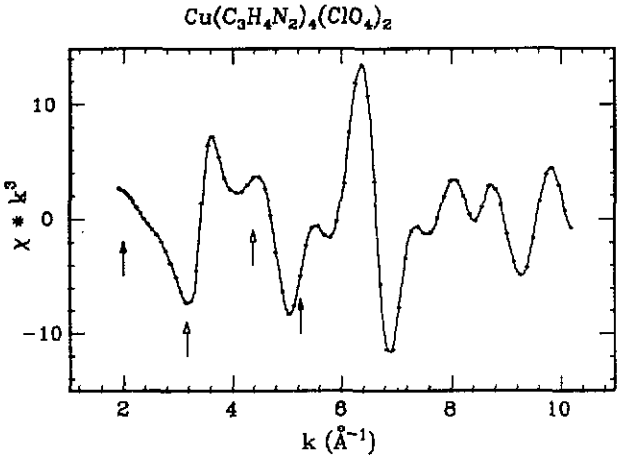

Figure 4. Total calculation for the EXAFS oscillation of the diperchlorato-tetraimidazolo-copper(II) molecule as a function of the photoelectron wavevector k (Å^{-1}) multiplied by k^3 to allow a comparison with typical experimental data. No thermal damping has been accounted for. The vertical arrows indicate the energies corresponding to the eigenvalue spectra reported in figure 5.

In this case a total calculation has been performed up to 30 Ryd above the edge which is a large number and many angular momenta ($l_{max}(\mathrm{Cu}) = 11$, $l_{max}(\mathrm{C,N}) = 7$) had to be included; consequently matrices larger then 1000×1000 had to be inverted. The recursion method can easily handle this.

Looking at the eigenvalue spectrum it is recognized that in the low energy part of the XAS spectrum the MS series is not convergent as some eigenvalues lie outside the circle, figure 5 (upper plots). At some intermediate energy figure 5 (lower plots) the eigenvalues are all within the circle, but some of them are still close to it reflecting the strong MS present in this molecular structure. At larger energies (not shown) the eigenvalue spectrum tends to collapse into the $(1, 0)$ point as it should do. The energies corresponding to the four plots of figure 5 are indicated in figure 4 by vertical

arrows. The number of iterations needed to reach convergence in the four cases were 13, 10, 9 and 8 as is also indicated in figure 5. We note that this scales approximately with the number of dangerous eigenvalues with respect to the broken line.

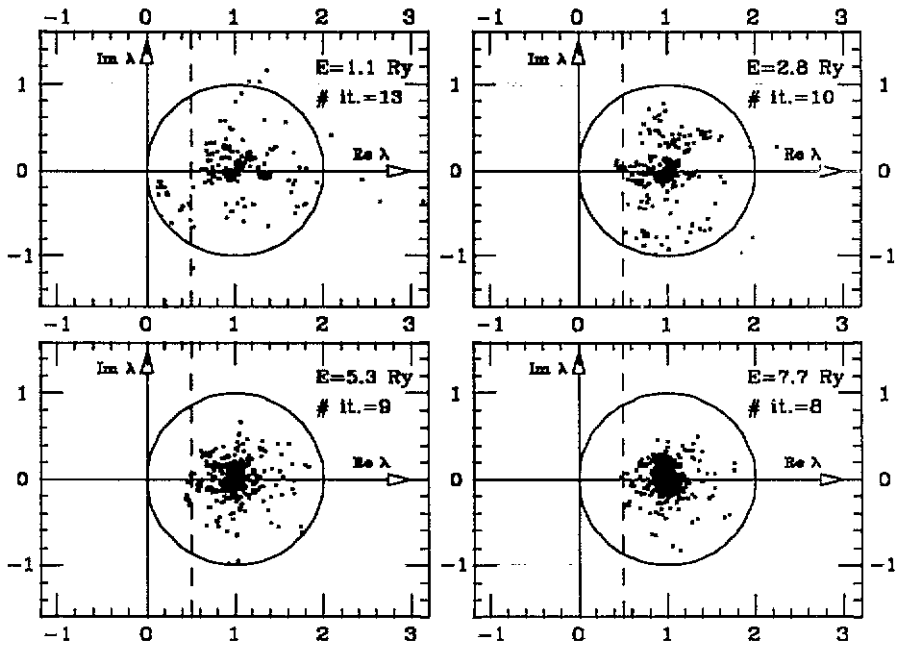

Figure 5. Eigenvalue spectra of the $I + GT$ matrix for the diperchlorato-tetraimidazolo-copper(II) molecule for four values of the energy, indicated in the upper right corners together with the number of iterations of the recursion needed for a relative error smaller than 10^{-5}. It is evident that the MS series does not converge at the first and second points. The recursion method converges instead in a small number of iterations.

The last application regards a calculation on a large cluster representative of a crystalline structure: c-Si, whose XAS spectrum has been widely studied for several fundamental reasons [21, 22]. Clusters of increasing size were chosen to see the effects of successive neighbouring shells. These were 47 atoms to include the first six shells around a central silicon atom, 71 atoms (seven shells) and 99 atoms (eight shells). The spectra, calculated with the recursion method iterated until convergence was reached, are reported in figure 6 with dotted, broken and full line patterns for the three sizes respectively. The zero energy scale is arbitrary. No thermal damping and core–hole broadening have been included. The imaginary part of the Hedin–Lundqvist interstitial potential starts to be non-zero at the energy of 0.4 Ryd and rises to 0.24 Ryd in the energy interval 2–4 Ryd of the spectrum; finally it decreases to 0.20 Ryd at 8 Ryd. This, which produces the main part of the energy-dependent broadening of the spectrum, roughly corresponds to a mean free path of the order of the distance of the boundary shells.

As a function of the energy, the number of iterations required for the convergence was greater in this last case than in the previous cases. This is somehow expected due to the large number of atoms in the structure. Around 100 steps were needed

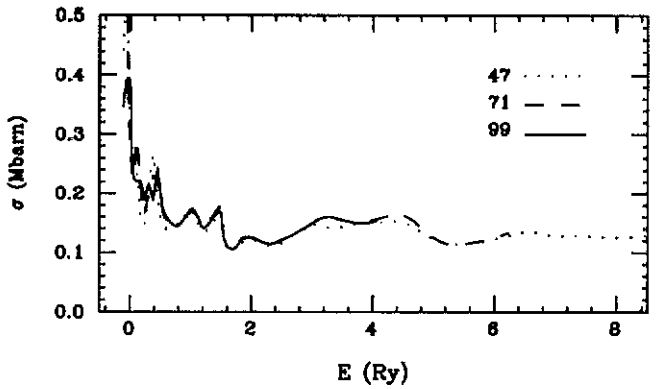

Figure 6. Cross-section calculations for c-Si using finite clusters of 47 (dots), 71 (dashes), and 99 (solid line) atoms. 99 atoms are necessary to reproduce correctly the first 1 Ryd of the spectrum.

at the beginning of the spectrum, while 10–15 were sufficient in the high energy part (5 Ryd above the edge). It should be noted, however, that results accurate to 1% are obtained with a one-tenth of the previously mentioned number of iterations.

Above the energy of 1 Ryd the spectrum of the 99-atom cluster coincides with the 71-atoms, that is seven shells are found to be sufficient to allow the spectrum to converge to its true crystalline shape. In an analogous way, above 5 Ryd six shells are sufficient. With 99 atoms the near-edge shape starts to be correctly reproduced [22]. The comparison with experiment [21] shows an overall agreement, even though some features like the peak at 3.3 Ryd and the structures around 1.6 Ryd are too sharp. This is tentatively attributed to a lack of thermal damping and core–hole width, although many-body effects could be also present.

The size of the matrices to be inverted was again larger than 1000 × 1000 due to the large number of atoms. The angular momenta limits were 3, 4 and 5 for the 99, 71 and 47 atoms calculations respectively.

The eigenvalue spectrum of the $I + GT$ matrix for 99 atoms at the energy of 0.467 Ryd corresponding to the first relevant peak in the near-edge region is shown in figure 7. The eigenvalues seem to group around a circular arc on the upper left side of the $(1, 0)$ point, which could be a sign of the tendency to coalesce into a cut in the limit of infinite number of atoms, and spread out of the circle of radius 1 along the other directions. The MS series is clearly not convergent; the CF algorithm instead required around 60 iterations in agreement with the number of dangerous eigenvalues.

This application shows how the recursion method works efficiently even in the case of strongly coupled matrices like those of large clusters, and in general may cover all of the structures that, in practice, scientists deal with.

4. Conclusions

In this paper the Haydock recursion scheme is applied for the first time to the inversion of the matrix $I+GT$ appearing in the calculation of the x-ray absorption cross section. Both qualitative arguments and numerical applications support the evidence for an

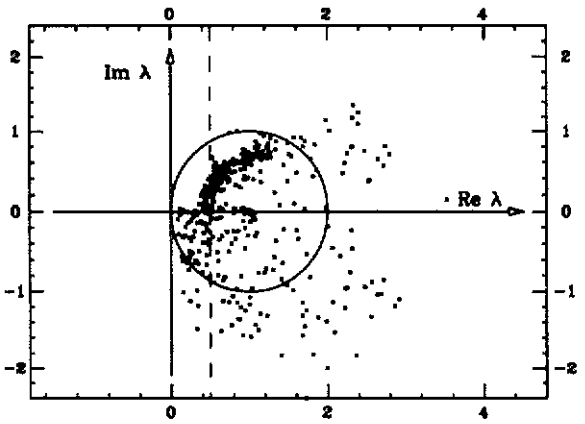

Figure 7. Distribution of the eigenvalue spectrum for the c-Si case (99-atom cluster) at the energy of 0.48 Ryd. Here around 60 iterations are required with the CF approach, while the MS series is clearly not convergent at all.

improved convergence with respect to the standard MS series. For this reason the proposed algorithm may have interesting applications.

The recursion method has been used numerically to perform the exact inversion of the $I + GT$ matrix, e.g. in typical XANES calculations, in the case of very different systems which cover most of the usual fields of applications. The energy range of the calculation, however, has been extended well beyond the XANES region and in the case of the copper-imidazole molecule up to nearly 30 Ryd above the edge. In a very recent paper [18] the method has been used to calculate signals associated with particular n-body arrangements in the framework of a new method of analysis of the XAS signals.

The analytic application of the recursion method, developed in section 2.2, has provided explicitly a mapping of the terms of the MS series into CF coefficients that improves the convergence of the calculation. Thus instead of using the usual MS terms χ_n it is proposed to use the CF approximants f_n whose analytic expression as a function of the related ξ_n quantities was given in section 2.3 equation (21). In the case of the MnO_6 complex, for instance it is found that f_3 is sufficient to reproduce all of the spectrum correctly. The analytic approximants (21) could be used as starting points to perform further manipulations like, for instance, to calculate analytically configurationally averaged cross sections.

The theory presented in this paper represents a bridge between the high energy EXAFS regime and low energy XANES regime that may be of interest in many fields of application.

Acknowledgments

Particular thanks for stimulating discussions are due to C R Natoli (INFN-Frascati) and A Di Cicco, Università di Camerino, Italy. The support of the personnel and computer time allocation at the 'Centro di Calcolo-Facoltà di Scienze and INFN-Università degli Studi dell' Aquila' is kindly acknowledged. This work has been partly supported by the National Organization for the Welfare of the Academic Research.

References

[1] Lagarde P, Raoux D and Petiau J 1986 *Proc. EXAFS and Near Edge Structure IV Conf.; J. Physique Coll.* **47** C8

[2] Chou S H, Rehr J J, Stern E A and Davidson E R 1987 *Phys. Rev.* B **35** 2604
Lu Dan and Rehr J J 1988 *Phys. Rev.* B **37** 6126

[3] Natoli C R, Benfatto M, Brouder C, Ruiz López M F and Foulis D L 1990 *Phys. Rev.* B **42** 1944

[4] Lee P A, Citrin P, Eisenberger P and Kincaid B 1981 *Rev. Mod. Phys.* **53** 769

[5] Durham P J, Pendry J D and Hodges C H 1981 *Solid State Commun.* **38** 159

[6] Lee P A and Pendry J B 1975 *Phys. Rev.* B **11** 2795

[7] Schaich W L 1984 *Phys. Rev.* B **29** 6513

[8] Benfatto M, Natoli C R, Bianconi A, Garcia J, Marcelli A, Fanfoni M and Davoli I 1986 *Phys. Rev.* B **34** 5774

[9] Durham P J, Pendry J B and Hodges C H 1982 *Comput. Phys. Commun.* **25** 193
Vvedensky D D, Saldin D K and Pendry J B 1986 *Comput. Phys. Commun.* **40** 421

[10] Filipponi A, Di Cicco A, Benfatto M and Natoli C B 1990 *Europhys. Lett.* **13** 319

[11] Haydock R, Heine V and Kelly M J 1972 *J. Phys. C: Solid State Phys.* **5** 2845; 1975 *J. Phys. C: Solid State Phys.* **8** 2591
Haydock R, Heine V, Kelly M J and Pendry J B 1972 *Phys. Rev. Lett.* **29** 868

[12] Heine V, Haydock R and Kelly M J 1980 *Solid State Physics* vol 35, ed H Ehrenreich, F Seitz and D Turnbull (New York: Academic)

[13] Evans M W, Grigolini P and Pastori Parravicini G 1985 *Memory Function Approaches to Stochastic Problems in Condensed Matter (Advances in Chemical Physics LXII)* (New York: Wiley)

[14] Lanczos C 1952 *J. Res. NBS* **45** 255; 1952 *J. Res. NBS* **49** 33

[15] Heine V, Haydock R and Kelly M J 1980 *Solid State Physics* vol 35, ed H Ehrenreich, F Seitz and D Turnbull (New York: Academic) p 310–11
Evans M W, Grigolini P and Pastori Parravicini G 1985 *Advances in Chemical Physics* vol LXII (New York: Wiley) p 145

[16] Heine V, Haydock R and Kelly M J 1980 *Solid State Physics* vol 35, ed H Ehrenreich, F Seitz and D Turnbull (New York: Academic) p 91

[17] Jones W B and Thron W J 1980 Continued Fractions *Encyclopedia of Mathematics and its Applications* vol 11, ed G C Rota (London: Addison-Wesley)

[18] Filipponi A, Di Cicco A, Tyson T A and Natoli C R 1991 *Solid State Commun.* **78** 265

[19] Sánchez del Río M, García J, Burattini E, Benfatto M and Natoli C B 1990 *Conf. Proc. Vol 25, 2nd European Conf. on Progress in X-Ray Synchrotron Radiation Research* ed A Balerna, E Bernieri and S Mobilio (Bologna: SIF) p 35

[20] Strange R W, Blackburn N J, Knowles P F and Hasnain S S 1987 *J. Am. Chem. Soc.* **109** 7157

[21] Bianconi A, Di Cicco A, Pavel N V, Benfatto M, Marcelli A, Natoli C R, Pianetta P and Woicik J 1987 *Phys. Rev.* B **36** 6426

[22] Sainctavit P, Petiau J, Benfatto M and Natoli C R 1990 *Conf. Proc. Vol 25, 2nd European Conference on Progress in X-Ray Synchrotron Radiation Research* ed A Balerna, E Bernieri and S Mobilio (Bologna: SIF) p 31